IOPscience iopscience.iop.org

Home Search Collections Journals About Contact us My IOPscience

Electrical resistivity of Cu and Nb thin films

This article has been downloaded from IOPscience. Please scroll down to see the full text article.

1998 J. Phys.: Condens. Matter 10 1707

(http://iopscience.iop.org/0953-8984/10/8/007)

View the table of contents for this issue, or go to the journal homepage for more

Download details:
IP Address: 171.66.16.209
The article was downloaded on 14/05/2010 at 12:19

Please note that terms and conditions apply.

J. Phys.: Condens. Matter **10** (1998) 1707–1720. Printed in the UK PII: S0953-8984(98)88705-5

Electrical resistivity of Cu and Nb thin films

M Fenn†, G Akuetey and P E Donovan

Department of Physics, Birkbeck College, University of London, London WC1E 7HX, UK

Received 27 October 1997

Abstract. The electrical resistivity and temperature coefficient of resistivity (TCR) of Cu and Nb thin films have been measured over a range of layer thicknesses between 5.6 nm and 1106 nm. The structure of the films has been characterized using transmission electron microscopy (TEM) and x-ray diffraction. The experimental results have been compared with the semi-classical theory of thin-film resistivity due to Dimmich. The grain boundary reflectivity, R, has been found to vary with grain size in the Nb films.

Dimmich's theoretical expression for the TCR does not match experiment, but by adapting the theoretical treatment a satisfactory fit has been obtained. The semi-classical expression predicts a negative TCR for certain thin-film and multilayer systems without the need to appeal to localization or correlation.

1. Introduction

The continuing interest in metallic single thin films and multilayers is motivated by their structural, optical, magnetic and transport properties that are unusual when compared with those of bulk materials. The transport properties with which we are currently concerned are interesting since they are fundamental properties of a metal and have relevance for the commercially important phenomena of magnetoresistance and giant magnetoresistance.

Experimentally, it is found that in a thin metal film the resistivity increases and the temperature coefficient of resistivity (TCR) decreases as the thickness of the metal layer is reduced. For very thin films the TCR can become negative (sometimes described as 'non-metallic' TCR although the TCR of a true non-metal has a different temperature dependence [2]). Many experimental investigations of these phenomena have been undertaken over the years, but most have concentrated on the resistivity or TCR alone, and systematic investigations of both are relatively rare.

The resistivity of thin films has been analysed theoretically using both quantum mechanical and semi-classical treatments. Quantum mechanical approaches are usually based on the Kubo–Greenwood formalism [3, 4], or (in the case of negative TCR) localization [5] and correlation [6]. Zhang and Butler [7] have noted that usable results derived from the Kubo–Greenwood formalism are greatly simplified and therefore, in the case of resistivity measured in the plane of the film, similar to the results of semi-classical theories. Semi-classical approaches are all based on solutions to the Boltzmann transport equation (see e.g. [8]). Following the original semi-classical solution for a thin metal film given by Fuchs and Sondheimer [9, 10], there have been a succession of improvements and adaptations by a number of workers, notably the introduction of crystal grain boundary scattering by Mayadas and Shatzkes [11–13].

† Now at: Department of Materials, University of Oxford, Parks Road, Oxford OX1 3PH, UK.

0953-8984/98/081707+14$19.50 © 1998 IOP Publishing Ltd

To our knowledge experimentalists have invariably compared their resistivity results with one of the available semi-classical theories. Those workers investigating the TCR have analysed their results in terms of localization [14, 15], localization and correlation [16], or the TCR predicted by semi-classical theory [17, 18]. Generally, the semi-classical theories have been found to overestimate the TCR.

We are investigating the resistivity and TCR of Cu and Nb thin films and Cu/Nb multilayers. Our results for Cu/Nb multilayers will be reported elsewhere. We report here our results for Cu and Nb single films, which have been compared with the predictions of the semi-classical theory due to Dimmich [1]. Dimmich's theory of transport in polycrystalline films and multilayers is both comprehensive and accessible to the experimentalist because it contains no undefined parameters or functions.

2. Dimmich's theory of thin-film electrical resistivity and TCR

Dimmich's expressions for the resistivity, ρ, and TCR, α, of a metallic multilayer are formulated in terms of the measurable parameters of bulk resistivity, bulk TCR, layer thickness and average grain diameter. The bulk mean free path or the mean free path ratio of the two metals is also required. In addition there are two adjustable parameters: p, the layer surface transmission parameter, and, R, the grain boundary reflectivity. The p-parameter can take values from zero (incoherent transmission) to 1 (coherent transmission), while the R-parameter can take values from zero (no reflection) to 1 (total reflection). Separate parameters are used for each metal in the multilayer. Dimmich [1] suggests that measurements on single films of each metal be made to determine values for R for use in the multilayer calculations. Dimmich's theory can be used to calculate the resistivity and TCR of single films, instead of multilayers, by setting the parameters of the two metals in the theory to those of the single metal in the film.

The input values to the expressions for metals 1 and 2 are:

bulk resistivity	$\rho_{01,02}$ (measured);
bulk TCR	$\alpha_{01,02}$ (measured);
grain boundary reflectivity	$R_{1,2}$ (to be found);
surface transmission	$p_{1,2}$ (assumed, see below);
layer thickness	$d_{1,2}$ (measured);
effective electron mass	$m_{1,2}$ (assumed $= m_e$, the free-electron mass);
bulk mean free path	$\lambda_{1,2}$ (calculated, see below);
average grain diameter	$b_{1,2}$ (measured).

For the bulk mean free path we have chosen to take the free-electron model value given by

$$\lambda = \frac{m_e v_F}{\rho n e^2}$$

where v_F is the Fermi velocity, n is the carrier density and the other symbols have their usual meanings. We use values of v_F and n from [19], and calculate the mean free path at the temperature at which we have measured the resistivity (273 K), giving 38.3 nm for Cu and 5.8 nm for Nb.

Dimmich's expression for ρ is

$$\frac{\rho}{\rho_0} = \frac{1 + h\gamma}{M_1 + h\gamma M_2}$$

where

$$M_1(k_{1,2}, p_{1,2}, l_{1,2}, R_{1,2}) = P(\alpha_1) - \frac{6}{\pi k_1}\int_0^{\pi/2} \mathrm{d}\varphi \int_0^1 \mathrm{d}t\, \frac{\cos^2\varphi}{H_1^2(t,\varphi)}(t-t^3)\left(1-\exp\left(-\frac{k_1 H_1(t,\varphi)}{t}\right)\right) \times \frac{1-p_2/c+p_2(1/c-p_1)\exp(-k_2H_2(t,\varphi)/t)}{1-p_1p_2\exp[-(k_1H_1(t,\varphi)+k_2H_2(t,\varphi))/t]}$$

$$M_2(k_{1,2}, p_{1,2}, l_{1,2}, R_{1,2}) = P(\alpha_2) - \frac{6}{\pi k_2}\int_0^{\pi/2} \mathrm{d}\varphi \int_0^1 \mathrm{d}t\, \frac{\cos^2\varphi}{H_2^2(t,\varphi)}(t-t^3)\left(1-\exp\left(-\frac{k_2 H_2(t,\varphi)}{t}\right)\right) \times \frac{1-p_1c+p_1(c-p_2)\exp(-k_1H_1(t,\varphi)/t)}{1-p_1p_2\exp[-(k_1H_1(t,\varphi)+k_2H_2(t,\varphi))/t]}$$

$$h = d_2/d_1 \qquad \gamma = \rho_{01}/\rho_{02} \qquad k_{1,2} = d_{1,2}/\lambda_{1,2}$$

$$l_{1,2} = b_{1,2}/\lambda_{1,2} \tag{1}$$

$$P(\alpha_{1,2}) = 1 - \frac{3}{2}\alpha_{1,2} + 3\alpha_{1,2}^2 - 3\alpha_{1,2}^3\ln(1+1/\alpha_{1,2})$$

$$\alpha_{1,2} = \frac{\lambda_{1,2}}{b_{1,2}}\frac{R_{1,2}}{1-R_{1,2}} \tag{2}$$

$$H_{1,2}(t,\varphi) = 1 + \frac{\alpha_{1,2}}{\cos\varphi(1-t^2)^{1/2}}$$

$$c = \frac{\lambda_1}{\lambda_2}\frac{m_2}{m_1}\frac{H_2(t,\varphi)}{H_1(t,\varphi)} \qquad \rho_0 = \frac{d\rho_{01}}{d_1+d_2\gamma} \qquad d = d_1 + d_2.$$

Dimmich's expression for the TCR, α, is given by

$$\alpha = \frac{M_1}{M_1+h\gamma M_2}\left[\alpha_{01}\left(1 - \frac{k_1}{M_1}\frac{\partial M_1}{\partial k_1} - \frac{l_1}{M_1}\frac{\partial M_1}{\partial l_1} + \frac{c}{M_1}\frac{\partial M_1}{\partial c}\right) - \alpha_{02}\left(\frac{k_2}{M_1}\frac{\partial M_1}{\partial k_2} + \frac{l_2}{M_1}\frac{\partial M_1}{\partial l_2} + \frac{c}{M_1}\frac{\partial M_1}{\partial c}\right)\right] + \frac{h\gamma M_1}{M_1+h\gamma M_2}\left[\alpha_{02}\left(1 - \frac{k_2}{M_2}\frac{\partial M_2}{\partial k_2} - \frac{l_2}{M_2}\frac{\partial M_2}{\partial l_2} - \frac{c}{M_2}\frac{\partial M_2}{\partial c}\right) - \alpha_{01}\left(\frac{k_1}{M_2}\frac{\partial M_2}{\partial k_1} + \frac{l_1}{M_2}\frac{\partial M_2}{\partial l_1} - \frac{c}{M_2}\frac{\partial M_2}{\partial c}\right)\right]$$

where $l_{1,2}$ (equation (1)) must be substituted into the expression for $\alpha_{1,2}$ (equation (2)) to perform the differentiation.

We have evaluated these integrals numerically using a simple rectangle method with a step size of 0.01 for t and φ, and for the differentiations a step of 0.001 in the form

$$\frac{\mathrm{d}f}{\mathrm{d}x} = \frac{f(x+\text{step}) - f(x)}{\text{step}}.$$

We find that these values replicate the graphical data in Dimmich's paper exactly.

In our investigations we have found that the theory for single films is much more sensitive to the value of R than it is to the value of p. Given the experimental uncertainties, we cannot justify extracting the value of p, so we have arbitrarily fixed it at the central value of 0.5 in all the subsequent analysis. We find that other values for p change the value of R by much less than the uncertainty in R for single films. We do have evidence that p

becomes important in multilayer calculations when the component layers are thin, and this will be discussed in a forthcoming publication.

3. Experimental method

3.1. Preparation of thin films and multilayers

The thin-film and multilayer specimens were deposited by DC magnetron sputtering in a UHV chamber with base pressure below 5×10^{-11} mbar. Multilayer samples were prepared to help in calibrating the deposition rates for the films described in this paper. The base pressure was measured using a VG Quadrupole Masstorr 100DX mass spectrometer, which showed that the principal residual gases in the chamber were molecular hydrogen and carbon monoxide. Deposition was carried out in high-purity argon at a pressure of 3×10^{-2} mbar. A single charge of argon was admitted to the chamber and pre-sputtering was carried out for 10 minutes in order to clean the target surfaces and to remove any reactive impurities from the argon atmosphere before the substrates were exposed to the metal vapour. Cu and Nb sputter targets of area 1500 mm^2 were cut from metal sheet purchased from Johnson–Matthey (Cu) and Goodfellow (Nb). The Cu target was 2 mm thick and the Nb 1 mm thick. The supplier's stated purities for the sheets were 99.999% (Cu) and 99.8% (Nb).

Specimens for resistivity measurements and x-ray characterization were deposited onto Pyrex substrates 3 mm $\times$ 15 mm $\times$ 1 mm thick. All of the substrates were thoroughly cleaned before film deposition, first in detergent, then in dilute nitric acid and finally with Analar grade propan-2-ol in a Sohxlet apparatus. All substrates were then coated with a thin (about 0.5 nm) film of evaporated pure amorphous carbon in a vacuum system at a pressure of $\sim 10^{-5}$ mbar. This carbon film acts as a wetting agent for the metal, promoting uniform film growth, and we find that the structure and conductivity of the films is always improved by this method. Specimens for TEM examination were deposited directly onto amorphous carbon support films mounted on 3 mm diameter microscope grids.

Electrical contact wires for resistance measurement specimens were mounted on the cleaned glass substrates before deposition of the film. Four bare copper wires 120 μm in diameter were glued directly to the glass with Degussa conductive adhesive, which has a specification of 10 $\mu\Omega$ cm volume resistivity. The voltage-measuring leads were approximately 10 mm apart and the current-carrying leads approximately 14 mm apart. The contacted substrates were left to dry overnight at ambient temperature, and then baked at 200 °C for 3.5 hours to cure the glue. Finally the substrates were coated with about 0.5 nm of pure carbon. The carbon film covered about 9 mm of the surface between the voltage leads, leaving $\sim$0.5 mm carbon-free surface next to each lead. The purpose of the carbon-free gap was to achieve an intimate contact between the film and the contacting wires.

The substrates were mounted on a computer-controlled rotating table, which could be positioned under each sputter target for a given time, following a pre-set sequence. The substrate table was fitted with shields to prevent cross-contamination during deposition. Two nominally identical specimens were prepared in each case in order to check the reproducibility of the experimental measurements.

The resistances of bulk Cu and Nb were measured using four contact wires spot-welded to specimens cut from the sheets. In order to convert the measured resistances to resistivities, the distance between the voltage measuring contacts on every specimen was measured using a vernier caliper, as was the thickness of the bulk specimens.

3.2. Thickness measurements on single films

The thicknesses of the single-film specimens were determined after deposition. Films of thickness greater than about 100 nm were measured using a Rank–Taylor–Hobson Talestep. Films of thickness less than 100 nm were measured by low-angle x-ray reflection using a Bede Scientific GXR1 reflectometer. The Kiessig fringes produced by interference between x-rays reflected from the top and bottom surface of the film were matched to computer simulations produced with the Bede REFS® software package. The simulations were used both to measure the film thickness and to provide an estimate of the rms roughness of the top and bottom surfaces.

The x-ray and Talestep thickness measurements on single films were used to calibrate the deposition rates for Cu and Nb. The deposition was found to be linear with time and highly reproducible from run to run. As an additional check, we prepared two series of multilayers, Gd/Nb and Cu/W, under exactly the same deposition conditions as were used for the Cu and Nb films and Cu/Nb multilayers. These systems have much higher x-ray contrast than Cu/Nb, so the low-angle x-ray patterns from these specimens could be used to measure the Cu and Nb deposition rates much more reliably. The results of these measurements confirmed the rate calibrations obtained from the single films at large (>5 nm) film thicknesses (i.e. long deposition times), and improved the calibration for small thicknesses, particularly in the case of the Cu, for which we had no single-film data at short deposition times because of the absence of Kiessig fringes from the thinner Cu films. The layer thicknesses of the Nb and Cu films were then checked using the multilayer calibrated deposition rates. The estimated uncertainty in the layer thicknesses determined in this way is 5%.

The uniformity of deposition over the area on the table occupied by the substrates was checked by optical transmission measurements on several films of different thicknesses. These showed a maximum variation in thickness of 5% between the two nominally identical specimens deposited in the same run.

3.3. Structural characterization

The internal structure of Nb and Cu films was investigated by plan-view transmission electron microscopy (TEM) in a JEOL 1200EX electron microscope. TEM was used to measure the average in-plane crystal diameter within the films as a function of film thickness, and also to check for the presence of preferred crystal orientation (texture) and oxidation.

The average crystal diameter was measured from dark-field images formed either from the Nb 110 reflection or from the Cu 111 and 200 reflections together. Dark-field images provide a more reliable indication of crystal diameter than bright-field images, since each illuminated region is a direct image of a coherently diffracting region. The average crystal diameter was determined with a calibrated optical viewer, measuring a random sample of 24 grains using an overlay grid on each TEM image

The degree of oxidation was assessed by observing the relative intensities of the diffraction from the metal and from its oxide in selected-area diffraction patterns. The films were checked for preferred orientation by observing the diffraction pattern while tilting the specimen in the microscope.

The surface of the films and the geometry of the contacts was investigated for a selection of the specimens using a JEOL 35CF scanning electron microscope (SEM).

3.4. Electrical resistance measurement

For resistance measurements the sample was lowered into the cooling gas of a Dewar of liquid helium. The sample temperature was measured using a calibrated (1.5 to 325 K) carbon glass sensor in conjunction with a Lakeshore Temperature Controller DRC-93CA. The average of temperature readings taken before and after the resistance measurement was used as the nominal temperature for a data point. For temperatures above room temperature, the sample could be warmed using a wire-wound heater.

The measuring current was supplied by a Keithley Model 220 Programmable Current Source using current reversal at 1 mA to minimize thermal emf and Joule heating. There was no difference in the data when 10 mA was used. For the bulk samples a measuring current of 100 mA was used because of their very low resistances. The voltages across the sample were measured using a Keithley Model 181 digital voltmeter.

The temperature range covered was 4.2 to 310 K.

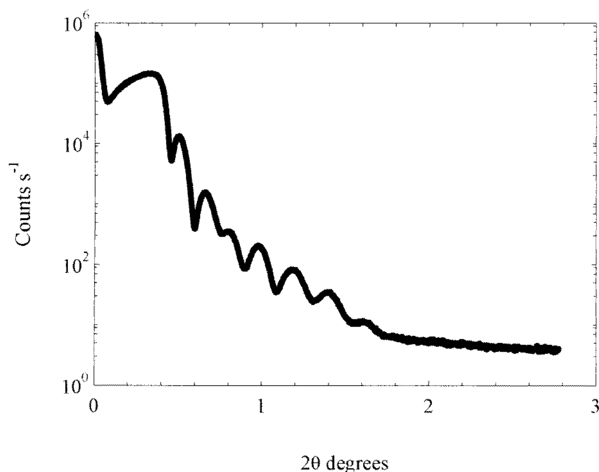

Figure 1. Kiessig fringes from a 21.5 nm Nb film with a 3.5 nm oxide overlayer.

4. Results

4.1. Thicknesses of single films

An example of the x-ray Kiessig fringes from a film of Nb is shown in figure 1. The fringes show a basic periodicity and an additional longer-period intensity modulation. The modulation indicates the presence of a second, thinner, continuous film on top of the Nb, which we assume to be native Nb oxide. Matching the observed pattern to REFS® simulations shows that the thickness of the oxide film is approximately 3.5 ± 0.3 nm and its density is (50 ± 5)% of the bulk density of Nb, giving a thickness lost to oxide of about 1.8 nm. This agrees with the published density of Nb oxide [20]. A comparable oxide film was observed on all the Nb single films x-rayed, and we have corrected for its presence when calculating their resistivity.

X-ray reflectivity measurements showed no evidence for a continuous native oxide layer on the Cu films. The Cu films produced good Kiessig fringes only over a restricted range of thickness. Cu films of less than 10 nm did not show fringes, suggesting either that the films

Table 1. Values for single-film thicknesses in nm. Each has an uncertainty of ±5%.

Cu	5.6	9.8	21	40	71	141	281	554	1106
Nb	2.5	4.2	6.7	11	20	33	68	148	288

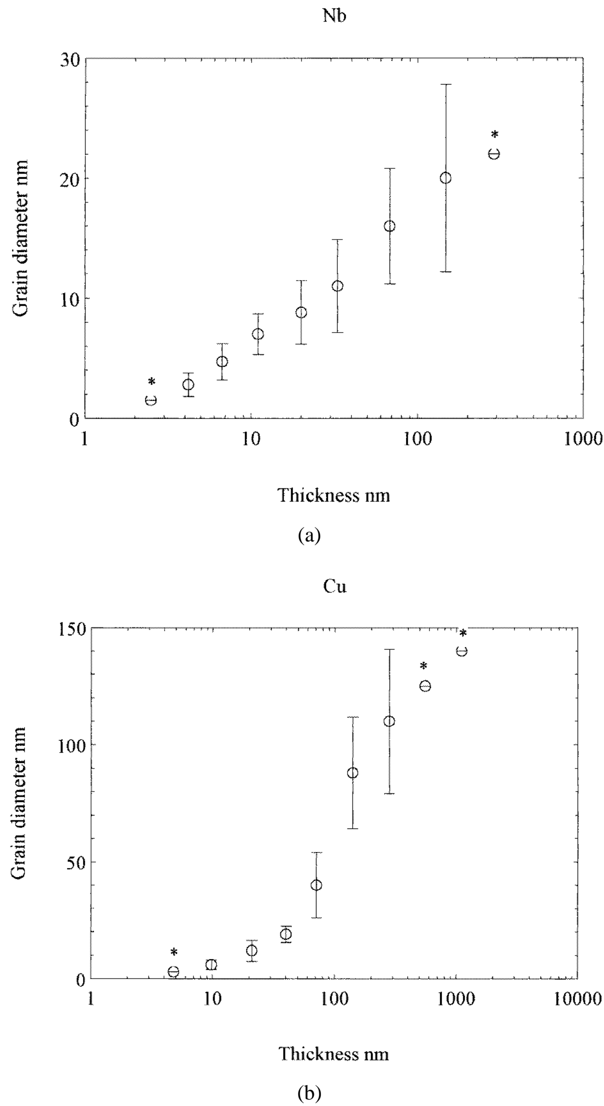

Figure 2. (a) Grain diameters for Nb single films. The error bars are ±1 standard deviation. Starred values are extrapolations. (b) Grain diameters for Cu single films. The error bars are ±1 standard deviation. Starred values are extrapolations.

have not formed as continuous layers or that the layers have broken up after deposition, perhaps because of oxidation. For Cu thicknesses greater than 40 nm the fringes are very rapidly damped with increasing angle of reflection, indicating that the film surface is rough.

In order to determine the thicknesses of the films which did not show Kiessig fringes we

calibrated the deposition rate of our system by means of x-ray reflectivity measurements on multilayer samples deposited under the same conditions (see section 3.2). The thicknesses of the films which could be measured directly from their Kiessig fringes agreed with the values calculated from the calibrated deposition rates in all cases. The deposition rates were 0.7 nm s^{-1} for Cu and 0.2 nm s^{-1} for Nb.

The thicknesses of the single films are given in table 1.

4.2. Structure of single films

TEM showed that both the Nb and the Cu films were polycrystalline. No preferred crystal orientation was observed in any of the specimens. In the case of Nb the intensities of the diffraction rings from Nb metal were always significantly greater than those of the oxide rings, even in the thinnest specimens, showing that the films were largely metallic even after exposure to the atmosphere. The measured dependence of Nb crystal diameter on film thickness is shown in figure 2(a).

In contrast to Nb, the Cu films were found to be significantly oxidized. For Cu films less than 25 nm thick the TEM images showed that the film had almost completely oxidized, forming relatively large (10 nm) oxide crystals and in the process breaking up into lumps. This observation agrees with the absence of Kiessig fringes in the x-ray diffraction patterns from Cu films of these thicknesses.

The observed oxidation of unprotected Cu single films meant that we could not use these films to determine the parameters b and R for Dimmich's theory. However, we found that it is possible to protect Cu films from oxidation by covering them with a thin Nb overlayer. We therefore made two additional series of plan-view TEM specimens, the first consisting of a Cu film with a 4.2 nm Nb overlayer and the second consisting of trilayers with the Cu sandwiched between two 4.2 nm Nb layers. We found that the presence of a Nb underlayer did not alter the crystal size or texture of the Cu. The dependence of Cu crystal diameter on film thickness determined from the protected and unprotected TEM specimens is shown in figure 2(b).

Both Cu and Nb films show an approximately linear variation of grain size with film thickness at small and large thicknesses, albeit with different slopes (this gives a sigmoidal shape on the logarithmic thickness scale shown in the figures). Hence a linear fit has been used to determine the grain sizes of very thin and very thick films, which cannot be successfully imaged with TEM without additional processing. Grain sizes determined by extrapolation are indicated in figures 2(a) and 2(b).

4.3. Electrical resistivity and TCR of single films

The resistivity results for single films of Cu and Nb at 273 K are shown in figures 3(a) and 3(b). It is not possible with our present apparatus to make resistivity measurements in vacuum, so we have to compensate as far as is possible for the effects of oxidation.

In calculating the resistivity of the Nb films, 1.8 nm has been subtracted from the total film thickness to allow for oxidation (see section 4.1), while the Cu thicknesses have not been adjusted.

Since we observed in TEM that thin Cu specimens were badly oxidized, we made a set of resistivity measurements on Cu films with protective Nb overlayers and underlayers and adjusted for the Nb resistivity. However the resistivities of these trilayer specimens were identical within uncertainty to that of the unprotected films of the same nominal thickness. Hence we did not consider it necessary to adjust the Cu thicknesses for oxidation.

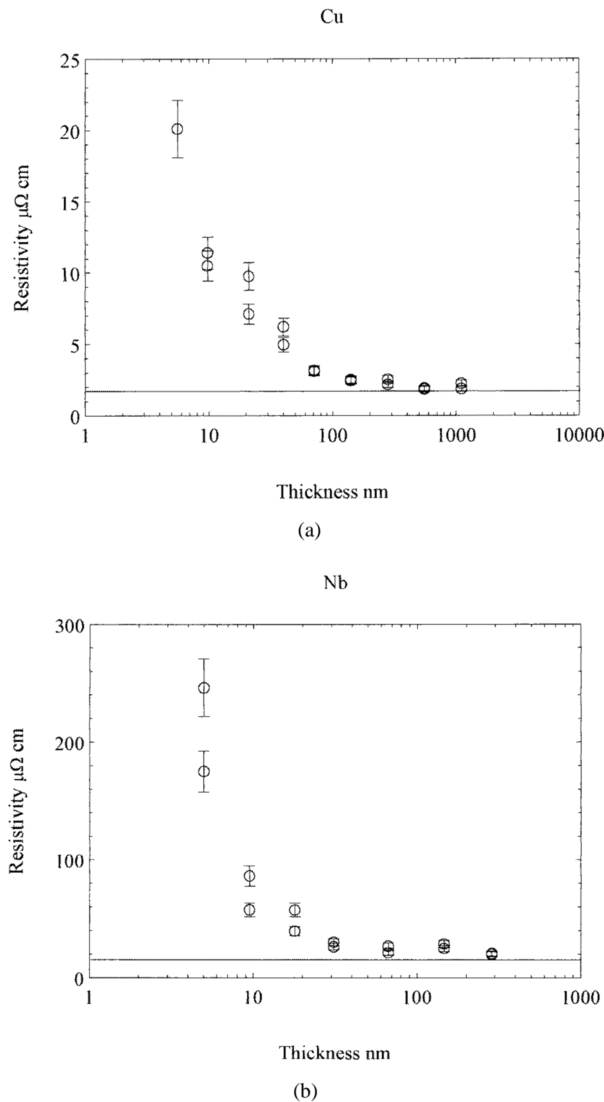

Figure 3. (a) The resistivity of Cu single-film sample pairs. One sample at 4.8 nm was damaged and so was not measured. The horizontal line is the measured bulk value of 1.72 $\mu\Omega$ cm. (b) The resistivity of Nb single-film sample pairs. The horizontal line is the measured bulk value of 15.2 $\mu\Omega$ cm. The Nb films at 2.5 nm and 4.2 nm did not conduct and have been omitted.

We observe increasing variation between the pair of nominally identical samples as the film thickness is reduced. Initially we suspected that the glued contacts might be responsible for some of this variation. The diameter of the contact wires is very much greater than the thickness of the deposited films, and we suspected that the thinnest films might not be forming a continuous layer across the glue and onto the wire. This problem would become more important as the thickness of the contact wire was increased. To investigate this we made eight samples of Nb films 5.0 nm thick (adjusted for oxidation), four of the samples with 120 μm diameter contact wire and four with 50 μm diameter contact wire. 50 μm wire was the thinnest that we were able to handle in our process. The samples with thinner

wire had an average resistivity of 199 $\mu\Omega$ cm and standard deviation 27 $\mu\Omega$ cm, while the samples with the thicker wire had an average resistivity of 237 $\mu\Omega$ cm and a standard deviation of 38 $\mu\Omega$ cm. These values agree within experimental uncertainty. Moreover, the lowest-resistivity sample in each set of four had the same resistivity. Hence we conclude that the contact wires are not the source of the variation. For the purposes of analysis we have used the results for the lowest-resistivity sample at each thickness.

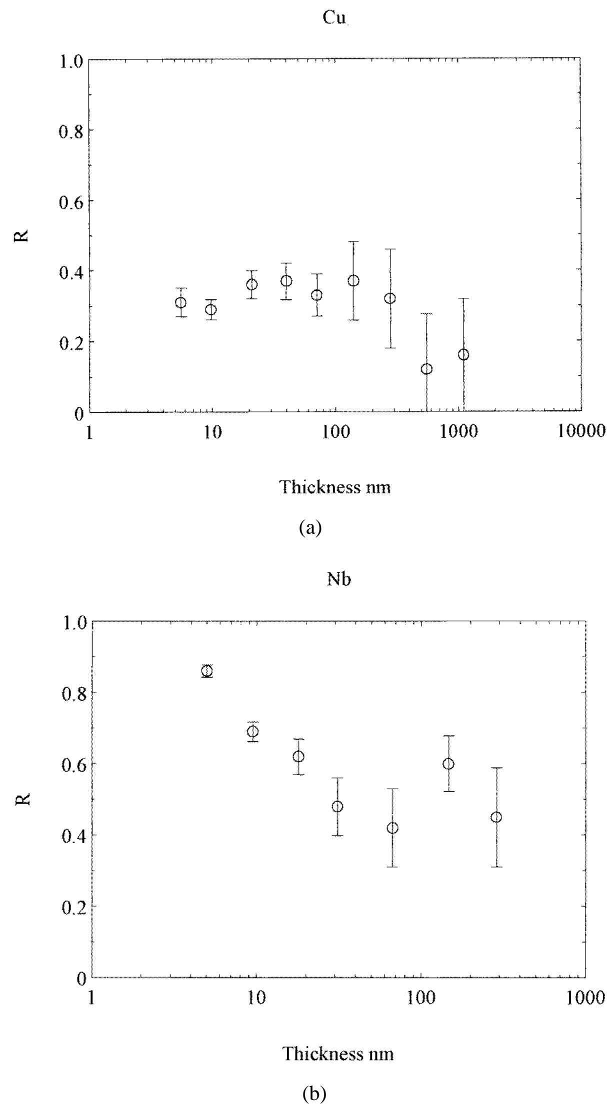

Figure 4. (a) Values for R for Cu single films. The error bars are those necessary to replicate the uncertainty in the resistivity. (b) Values for R for Nb single films. The error bars are those necessary to replicate the uncertainty in the resistivity.

We now have the components necessary to extract values for R for our single films using Dimmich's theory. The results are shown for Cu and Nb in figures 4(a) and 4(b).

It has usually been assumed that R is constant with film thickness, grain size and

temperature. However, our results indicate that R varies with grain size in Nb. Within experimental uncertainty, and giving extra weight to R-values determined using measured rather than extrapolated grain sizes, we can assign to Cu a constant value for R of about 0.35 for our single films. Given the uncertainty in R, this is comparable to other values in the literature including 0.24 [12], 0.3 [21] and 0.38 [22]. For thick Nb films R appears to be about 0.55, rising to 0.85 or more when the film is thinner than 10 nm. To our knowledge this is the first time a value for R for Nb has been obtained.

4.4. Single-film TCR

The TCR provides a useful check of Dimmich's theory since it requires no additional parameters other than the bulk TCR. Comparison of our experimentally measured TCR values with theory calculations showed that the theory overestimated the TCR by about a factor of 2 for the thicker films and by an even larger factor as the thickness was reduced, although as the TCR approaches zero at small thicknesses this is not readily apparent in a graph. We have checked the derivation of Dimmich's TCR expression and found it to be correct, so our initial speculation was that one of the supposedly temperature-independent parameters in the resistivity expression might in fact vary with temperature. Since the theory is most sensitive to the value of R we checked first for any variation in R with temperature by substituting values for bulk resistivity and mean free path appropriate to different temperatures into Dimmich's resistivity expression, and extracted the R-value which gave the single-film resistivity for that temperature. This showed R to be almost constant with temperature as is usually assumed, but gives an insight into the TCR discrepancy since it shows that, once R has been found for one temperature, Dimmich's resistivity expression gives the correct value of the resistivity over a wide range of temperatures. Since Dimmich's theory gives correct results for the resistivity at different temperatures, the TCR can be extracted in the same form as the experimental values:

$$\mathrm{TCR} = \frac{1}{\rho(78\ \mathrm{K})} \frac{\rho(273\ \mathrm{K}) - \rho(78\ \mathrm{K})}{273\ \mathrm{K} - 78\ \mathrm{K}}$$

using the calculated values of $\rho(273\ \mathrm{K})$ and $\rho(78\ \mathrm{K})$.

This is effectively extracting the TCR from Dimmich's resistivity expression adapted to the form $\rho(T)$. We measured the resistivity of both bulk metals at 78 K for our analysis and obtained the values 0.26 $\mu\Omega$ cm for Cu, giving a mean free path of about 260 nm, and 3.2 $\mu\Omega$ cm for Nb, giving a mean free path of about 28 nm. The values of the film TCR obtained are shown as $\rho(T)$ in figures 5(a) and 5(b) where they are compared with experiment and the values obtained from Dimmich's original expression for the TCR. The $\rho(T)$ fit is not perfect in that not all of the error bars intersect with those of the experimental values, but it is clearly a much better fit than Dimmich's original expression.

This raises a question as to why, if Dimmich's resistivity expression gives the correct temperature dependence, its temperature derivative does not. We suggest that the fault lies in the simplifying assumption used in the derivation of the TCR expression in [1]:

$$\frac{1}{\rho}\frac{\mathrm{d}\rho}{\mathrm{d}T} = -\frac{1}{\lambda}\frac{\mathrm{d}\lambda}{\mathrm{d}T}.$$

This assumption is equivalent to assuming $\rho\lambda$ = constant as predicted by the free-electron model. The suggestion has been made that polycrystalline thin films do not obey this relation due to the presence of grain boundaries [23] and hence the existence of more than one scattering length, requiring a more complex expression for the temperature coefficient. This suggestion might be tested by making TCR measurements on single-crystal films,

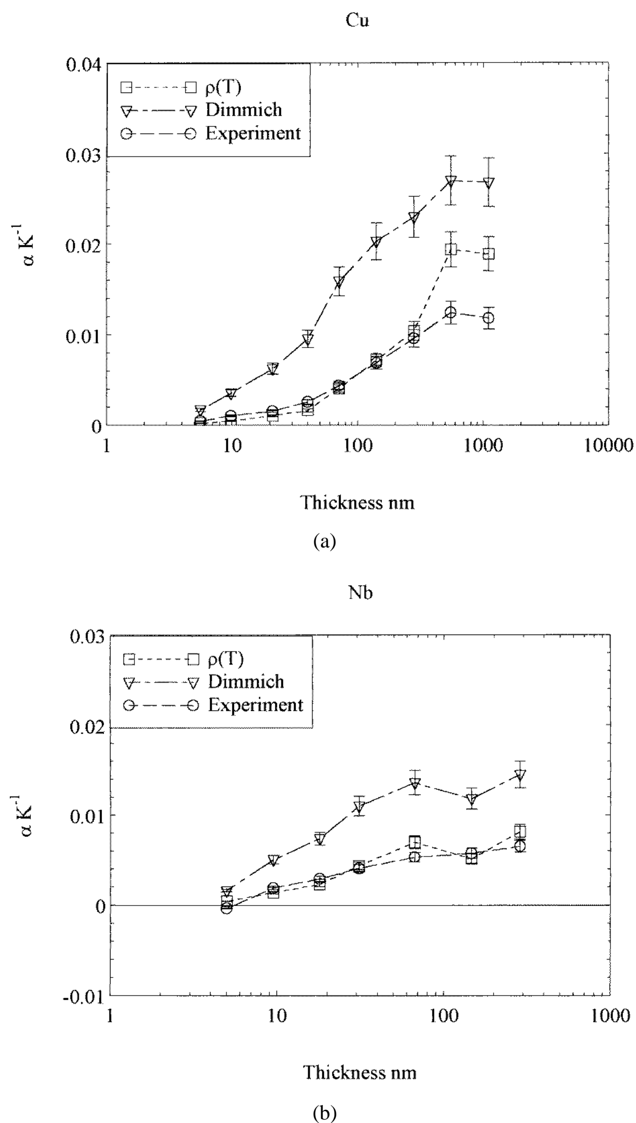

Figure 5. (a) Values for the TCR of Cu single films. The bulk TCR was 0.029 K^{-1}. (b) Values for the TCR of Nb single films. The bulk TCR was 0.019 K^{-1}.

where the absence of grain boundaries would be expected to make the values from the $\rho(T)$ and the original TCR expression coincide.

5. Conclusions

Dimmich's theory appears to provide a good description of the resistivity and TCR of metallic thin films. Our results for the grain boundary reflectivity, R, for Cu are consistent with a constant value of about 0.35. Our results for R for Nb are consistent with a constant value of about 0.55 at large layer thicknesses but with a substantial increase below a layer

thickness of 10 nm which corresponds to a grain size around 6 nm. This indicates that R can vary with grain size.

Dimmich's original expression for the TCR does not fit experiment, but by adapting the resistivity expression to different temperatures we have obtained a reasonable fit. This raises a question concerning the assumptions used to produce the expression for the TCR, and we suggest that the assumption $\rho\lambda =$ constant is incorrect, possibly because of grain boundary scattering. Measurements on single-crystal samples could be used to test this possibility.

Our simulations using Dimmich's equations also predict negative TCR in multilayers when physically realistic values of the parameters are used, so by repeating our experimental procedure with more resistive metals we hope to produce multilayers with strong negative TCR, and we are encouraged by our present TCR fit to believe that Dimmich's theory will predict these negative values correctly. If this is the case, it will suggest that it is not necessary to appeal to localization or correlation to explain the occurrence of negative TCR in metallic multilayers, and that this phenomenon emerges naturally from semi-classical theory.

The values of R determined in this investigation can be used in analysing the resistivity and TCR of Cu/Nb multilayers. This will be described in a forthcoming publication.

Acknowledgments

This research was supported by EPSRC (postgraduate studentship 95308257) and by Birkbeck College.

We are grateful to Dr S Zochowski for the design and construction of the resistance-measuring system.

We would like to thank Mr F Stride of University College, London, for measuring the thicknesses of the pure films, and Ms J Munn for assistance with the electron microscopy, which was carried out in the EM Unit of the Department of Crystallography, Birkbeck College.

We would also like to thank Degussa Limited for their donation of the contact adhesive.

References

[1] Dimmich R 1985 *J. Phys. F: Met. Phys.* **15** 2477
[2] Mott N F and Kaveh M 1985 *Adv. Phys.* **34** 329
[3] Kubo R 1957 *J. Phys. Soc. Japan* **12** 570
[4] Greenwood D A 1958 *Proc. Phys. Soc.* **71** 585
[5] Anderson P W 1958 *Phys. Rev.* **109** 1492
[6] Altshuler B L 1980 *Phys. Rev. Lett.* **44** 1288
[7] Zhang X G and Butler W H 1995 *Phys. Rev.* B **51** 10 085
[8] Ashcroft and Mermin 1976 *Solid State Physics* (Philadelphia, PA: Saunders College Publishing)
[9] Fuchs K 1938 *Proc. Camb. Phil. Soc.* **34** 100
[10] Sondheimer E H 1952 *Adv. Phys.* **1** 1
[11] Soffer S B 1967 *J. Appl. Phys.* **38** 1710
[12] Mayadas A F and Shatzkes M 1970 *Phys. Rev.* B **1** 1382
[13] Sambles J R, Elsom K C and Jarvis D J 1982 *Phil. Trans. R. Soc.* A **304** 365
[14] Fontana M P, Podini P, Jiang Zuimin and Liu Wen 1990 *Phys. Rev.* B **42** 5859
[15] Sousa J B, Pinto R P, Almeida B, Braga M E, Freitas P P, Melo L V and Trindade I G 1994 *J. Magn. Magn. Mater.* **137** 73
[16] Werner T R, Banerjee I, Yang Q S, Falco C M and Schuller I K 1982 *Phys. Rev.* B **26** 2224
[17] Izumiya T, Hanamure T, Saito E, Kaneko T and Yamamoto R 1990 *J. Phys.: Condens. Matter* **2** 1179
[18] Falco C M 1984 *J. Physique Coll.* **45** C5 499
[19] Kittel 1986 *Introduction to Solid state Physics* (New York: Wiley)

[20] Powder Diffraction File (JCPDS)
[21] Kaneko T, Sasaki T, Sakuda M, Yamamoto R, Nakamura T, Yamamoto H and Tanaka S 1988 *J. Phys. F: Met. Phys.* **18** 2053
[22] Artunç N and Öztürk Z Z 1993 *J. Phys.: Condens. Matter* **5** 559
[23] Vancea J, Hoffmann H and Kastner K 1984 *Thin Solid Films* **121** 201